Observation of the lead carbonyls, $Pb_nCO(n=1–4)$: Reactions of lead atoms and small clusters with carbon monoxide in solid argon

Ling Jiang, and Qiang Xu

Citation: The Journal of Chemical Physics **122**, 034505 (2005); doi: 10.1063/1.1834915
View online: https://doi.org/10.1063/1.1834915
View Table of Contents: http://aip.scitation.org/toc/jcp/122/3
Published by the American Institute of Physics

Observation of the lead carbonyls, Pb_nCO ($n=1-4$): Reactions of lead atoms and small clusters with carbon monoxide in solid argon

Ling Jiang and Qiang Xu[a)]
National Institute of Advanced Industrial Science and Technology (AIST), Ikeda, Osaka 563-8577, Japan and Graduate School of Science and Technology, Kobe University, Nada Ku, Kobe, Hyogo 657-8501, Japan

(Received 8 September 2004; accepted 27 October 2004; published online 28 December 2004)

Reactions of laser-ablated Pb atoms with CO molecules in solid argon lead to the formation of the lead carbonyls, Pb_nCO ($n=1-4$), using matrix-isolation infrared spectroscopy. Absorption at 2027.7 cm^{-1} is assigned to C–O stretching mode of the PbCO product, which appears and increases on annealing, disappears on broadband irradiation, and recovers on further annealing. Small lead cluster mono-carbonyls Pb_nCO ($n=2-4$) are also observed in the present infrared spectra. Based on the results of stepwise annealing and the comparison with theoretical predictions, the absorptions at 1915.5, 1923.8, and 2042.8 cm^{-1} are assigned to Pb_2CO, Pb_3CO, and Pb_4CO, respectively. Bridging CO is found in Pb_2CO or Pb_3CO, whereas terminal CO in Pb_4CO. The density functional theory calculations have been performed on these molecules and small naked lead clusters. The good agreement between experimental and calculated vibrational frequencies, relative absorption intensities, and isotopic shifts provides strong support for the identifications of these lead mono-carbonyls Pb_nCO ($n=1-4$). Furthermore, energetic analysis for the possible reactions of lead atoms with CO molecules is also given. © *2005 American Institute of Physics.*
[DOI: 10.1063/1.1834915]

I. INTRODUCTION

Reactions of carbon monoxide with atoms of main group elements as well as transition metals have been the topic of experimental and theoretical interest in recent years.[1–3] A good case in point is the investigation of the spectra, structures, and bonding of group 14 carbonyls.[4–16] The $M(CO)_n$ ($M=$C, Si, Ge, and Sn; $n=1$, 2) molecules have been obtained from the reactions of thermally evaporated or laser-ablated C, Si, Ge, and Sn atoms with CO molecules in low-temperature rare gas matrices.[5,15,16] In addition to these group 14 carbonyl neutrals, carbonyl anions such as $SiCO^-$, $GeCO^-$, and $SnCO^-$, all of which have triplet ground states with a linear geometry, have also been successfully synthesized.[5]

A variety of experimental and theoretical studies on group 14 clusters could be found in the literature.[17–21] The gas phase electronic spectra of Sn_2 and Pb_2 have been obtained by combining pulsed laser vaporization with laser induced fluorescence.[17] The vibrational frequency of Pb_2 has been reported to be 112 cm^{-1} in the $X(O_g^+)$ ground state in solid argon.[18] There have been a few experimental studies on charged lead clusters.[19] The photodetachment spectra of Sn_2^- and Pb_2^- clusters and mixed dimers have been studied and the results have been found to be in very good agreement with the previous theoretical calculations on Sn_2^- and Pb_2^-.[20] Moreover, the ground states of Ge_4, Sn_4, and Pb_4 have been calculated to be ^1A_g states with equilibrium geometries of rhombus similar to Si_4.[21]

Recently, the infrared spectra of Fe_2CO,[22–24] Co_2CO,[25] B_2CO,[26] and Si_nCO ($n=2-5$) (Ref. 27) have been reported. Theoretical investigations have been carried out for Fe_nCO ($n=1-6$),[28] Cu_nCO ($n=2-13$),[29] and Ni_2CO.[30] In contrast with considerable experimental and theoretical studies of the interactions of CO molecules with the transition metal and main group element atoms, however, almost none is known about the heavier lead carbonyl. Here, we report the observation of the lead carbonyls, Pb_nCO ($n=1-4$), generated from the reactions of lead atoms with CO molecules in solid argon using infrared spectroscopy. The density functional theory (DFT) calculations are performed to support the experimental assignments of the infrared spectra. We also make an attempt to elucidate the mechanisms for the possible reactions of CO molecules with lead atoms and clusters.

II. EXPERIMENTAL AND THEORETICAL METHODS

The experiment for laser ablation and matrix isolation infrared spectroscopy is similar to those reported previously.[31] The Nd:YAG (YAG—yttrium aluminum garnet) laser fundamental (1064 nm, 10 Hz repetition rate with 10 ns pulse width; Minilite II, Continuum) was focused on the rotating lead target. The laser-ablated lead atoms were codeposited with CO in excess argon onto a CsI window cooled normally to 7 K by means of a closed-cycle helium refrigerator (Cryotec, Daikin). The matrix gas deposition rate was typically of 2–4 mmol per h. Typically, 2–5 mJ/pulse

[a)]Author to whom correspondence should be addressed. Electronic mail: q.xu@aist.go.jp

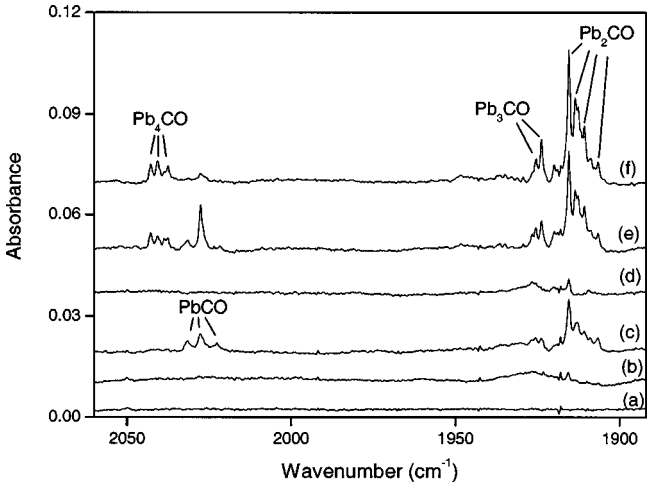

FIG. 1. Infrared spectra in the 2050–1900 cm^{-1} region from codeposition of laser-ablated Pb atoms (5.0 mJ/pulse) with 0.5% CO in Ar. (a) One hour of sample deposition at 7 K, (b) after annealing to 30 K, (c) after annealing to 34 K, (d) after 15 min of broadband irradiation, (e) after annealing to 38 K, and (f) after annealing to 40 K.

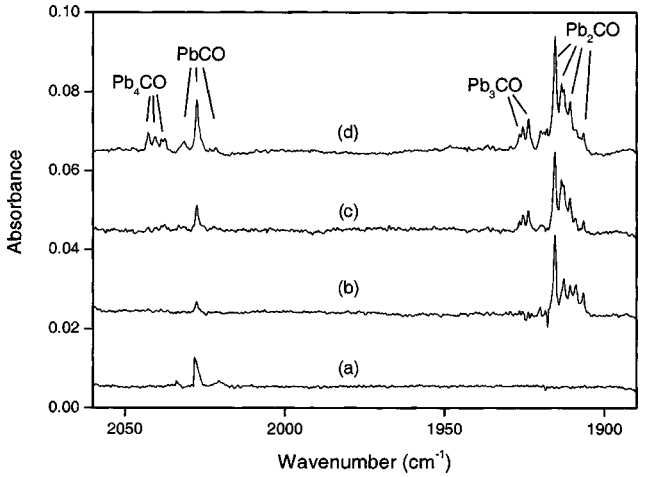

FIG. 2. Infrared spectra in the 2050–1900 cm^{-1} region from codeposition of laser-ablated Pb atoms with 0.5% CO in Ar after 15 min of UV irradiation and annealing to 38 K. Laser power (mJ/pulse): (a) 2.0, (b) 3.5, (c) 4.0, and (d) 5.0.

laser power was used. Carbon monoxide (99.95% CO, Japan Fine Products), $^{13}C\,^{16}O$ (99%, $^{18}O<1\%$, ICON), and $^{12}C\,^{18}O$ (99%, ICON) were used to prepare the CO/Ar mixtures. In general, matrix samples were deposited for 1–2 h. After sample deposition, IR spectra were recorded on a BIO-RAD FTS-6000*e* spectrometer at 0.5 cm^{-1} resolution using a liquid nitrogen cooled HgCdTe (MCT) detector for the spectral range of 5000–400 cm^{-1}. Samples were annealed at different temperatures and subjected to broadband irradiation ($\lambda > 250$ nm) using a high-pressure mercury arc lamp (Ushio, 100 W).

Quantum chemical calculations were performed to predict the structures and vibrational frequencies of the observed reaction products using the GAUSSIAN03 program.[32] To address the difference in CO binding energies for MCO (M=C, Si, Ge, Sn, and Pb) carbonyls, compared calculations were also carried out. The Becke three parameter hybrid functional with the Lee-Yang-Parr correlation corrections (B3LYP) was used.[33,34] The 6-311+G(d) basis sets were used for C, O, Si, and Ge atoms,[35] and the Los Alamos ECP plus DZ (LANL2DZ) were used for Sn and Pb atoms.[36,37] Geometries were fully optimized and vibrational frequencies were calculated with analytical second derivatives.

III. RESULTS AND DISCUSSION

Experiments have been done with carbon monoxide concentrations ranging from 0.2% to 2.0% in argon. Typical infrared spectra for the reactions of laser-ablated lead atoms with CO molecules in excess argon in the selected regions are shown in Figs. 1–3, respectively, and the product absorptions are listed in Table I. The stepwise annealing and photolysis behavior of the product absorptions is also shown in the figures and will be discussed below.

Quantum chemical calculations have been performed on the potential product molecules. The most stable structures optimized by hybrid B3LYP calculations for lead carbonyls are displayed in Fig. 4.[38] The ground states, point groups, vibrational frequencies, and intensities are listed in Table II. Table III presents a comparison of observed and calculated isotopic frequency ratios for the C–O stretching modes of the reaction products. Net charges of CO, selected bond lengths of M–C and C–O, and CO binding energies along with vibrational frequencies of C–O stretching mode are reported in Table IV. Energetic analysis for possible reactions of Pb atoms with CO molecules is given in Table V.

A. PbCO

The sharp band at 2027.7 cm^{-1} with two trapping sites at 2031.7 and 2022.7 cm^{-1} (Table I and Figs. 1–3) has been observed on sample annealing, destroyed on broadband irradiation, and reobserved on sample annealing. Interestingly, the relative yields of these bands sharply increased with higher CO concentration (i.e., 2.0%) and lower laser power (3 mJ/pulse). The 2027.7 cm^{-1} band shifts to 1983.9 cm^{-1}

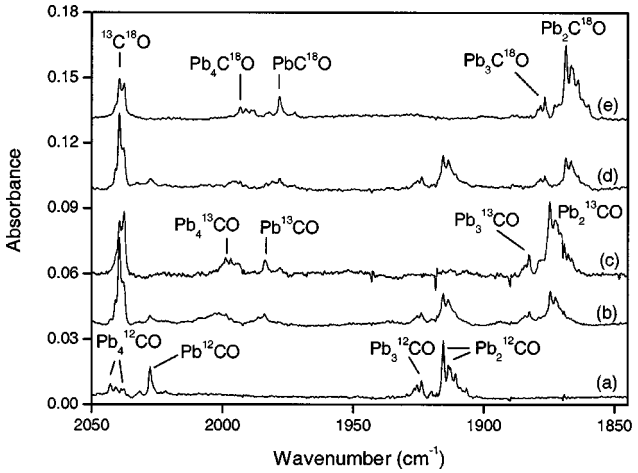

FIG. 3. Infrared spectra in the 2050–1850 cm^{-1} region for laser-ablated lead atoms codeposited with isotopic CO in Ar after 15 min of UV irradiation and annealing to 38 K. (a) 0.5% $^{12}C\,^{16}O$, (b) 0.25% $^{12}C\,^{16}O$ + 0.25% $^{13}C\,^{16}O$, (c) 0.5% $^{13}C\,^{16}O$, (d) 0.25% $^{12}C\,^{16}O$ + 0.25% $^{12}C\,^{18}O$, and (e) 0.5% $^{12}C\,^{18}O$.

TABLE I. Infrared absorptions (cm^{-1}) observed after codeposition of laser-ablated lead atoms with CO in excess argon at 7 K.

$^{12}C\,^{16}O$	$^{13}C\,^{16}O$	$^{12}C\,^{18}O$	$^{12}C\,^{16}O+^{13}C\,^{16}O$	$^{12}C\,^{16}O+^{12}C\,^{18}O$	$R(12/13)$	$R(16/18)$	Assignment
2042.8	1998.8	1993.2	2042.8, 1998.8	2042.8, 1993.2	1.0220	1.0249	Pb_4CO
2040.8	1996.8	1991.2	2042.8, 1996.8	2042.8, 1991.2	1.0220	1.0249	Pb_4CO site
2037.6	1993.4	1988.0	2037.6, 1993.4	2037.6, 1988.0	1.0221	1.0250	Pb_4CO site
2031.7	1987.7	1982.1	2031.7, 1987.7	2031.7, 1982.1	1.0221	1.0250	PbCO site
2027.7	1983.9	1978.2	2027.7, 1983.9	2027.7, 1978.2	1.0221	1.0250	PbCO
2022.7	1978.9	1973.4	2022.7, 1978.9	2022.7, 1977.3	1.0221	1.0250	PbCO site
1925.6	1884.4	1878.4	1925.6, 1884.4	1925.6, 1878.4	1.0219	1.0251	Pb_3CO site
1923.8	1882.7	1876.7	1923.8, 1882.7	1923.8, 1876.7	1.0218	1.0251	Pb_3CO
1915.5	1874.8	1868.6	1915.5, 1874.8	1915.5, 1868.6	1.0217	1.0251	Pb_2CO
1913.6	1872.8	1866.7	1913.6, 1872.8	1913.6, 1866.7	1.0218	1.0251	Pb_2CO site
1910.8	1870.3	1864.1	1910.8, 1870.3	1910.8, 1864.1	1.0217	1.0251	Pb_2CO site
1906.7	1866.1	1860.1	1906.7, 1866.1	1906.7, 1860.1	1.0218	1.0251	Pb_2CO site

with $^{13}C\,^{16}O$ and to 1978.2 cm^{-1} with $^{12}C\,^{18}O$. The mixed $^{12}C\,^{16}O+^{13}C\,^{16}O$ and $^{12}C\,^{16}O+^{12}C\,^{18}O$ isotopic spectra (Fig. 3) only provide the sum of pure isotopic bands, indicating that only one CO subunit is involved in this mode. The isotopic $^{12}C/^{13}C$ and $^{16}O/^{18}O$ ratios are 1.0221 and 1.0250, respectively, also indicating single CO involvement. Accordingly, the 2027.7 cm^{-1} band is assigned to the C–O stretching mode of PbCO.

The DFT calculations lend strong support for the assignment. PbCO is predicted to have a linear geometry (Fig. 4) with a $^3\Sigma^-$ ground state (Table II), which is in good agreement with the previous theoretical investigation.[5] The calculated C–O stretching mode of the PbCO species is 1999.8 cm^{-1} (Table II), which should be multiplied by 1.014 to fit the observed frequency. The calculated $^{12}C/^{13}C$ and $^{16}O/^{18}O$ isotopic frequency ratios of 1.0224 and 1.0252 are consistent with the experimental observations 1.0221 and 1.0250. At the B3LYP/6-311+G(*d*) level, the CO binding energies for CCO, SiCO, and GeCO carbonyl are 61.99, 36.56, and 27.93 kcal/mol, respectively. At the B3LYP/6-311+G(*d*)-LANL2DZ level, the CO binding energies for SnCO and PbCO are predicted to be 18.30 and 16.12 kcal/mol, respectively. That is to say, the dissociation of PbCO to Pb atom and CO molecule requires the smallest energy among the *M*CO (*M*=C, Si, Ge, Sn, and Pb) carbonyls. In fact, the present experiments show that the infrared absorptions of PbCO appear and increase on annealing, disappear on broadband irradiation, and recover on further annealing (Fig. 1), suggesting that the interaction of CO with Pb is not strong enough to resist the photoinduced dissociation as expected. The feature of photoinduced dissociation for other lighter *M*CO (*M*=C, Si, Ge, and Sn) carbonyls was not observed in the previous experiments.[5,15,16]

It appears that both the mono-carbonyl and the dicarbonyl absorptions are prominent for the Si, Ge, and Sn+CO systems,[5] and one might expect such a situation also to prevail for the Pb+CO system. However, the mixed isotopic substitution experiments on the 50% ^{13}C and ^{18}O enriched samples (Fig. 3) do not indicate the mixed isotopic characteristic of $Pb(CO)_2$ in the present work. There is one exception in which a prominent central peak for the mixed ^{12}C, ^{13}C or ^{16}O, ^{18}O dicarbonyl would not appear; the two CO-stretching vibrations would be decoupled if the CO bonds were perpendicular to one another. However, our DFT calculation of the geometry of $Pb(CO)_2$ shows that this situation does not arise, in agreement with the previous report.[5] Furthermore, the small reaction energy (−2.44 kcal/mol) calculated for the reaction, $PbCO+CO\rightarrow Pb(CO)_2$, accounts for the absence of the heavier $Pb(CO)_2$ absorptions (*vide infra*).

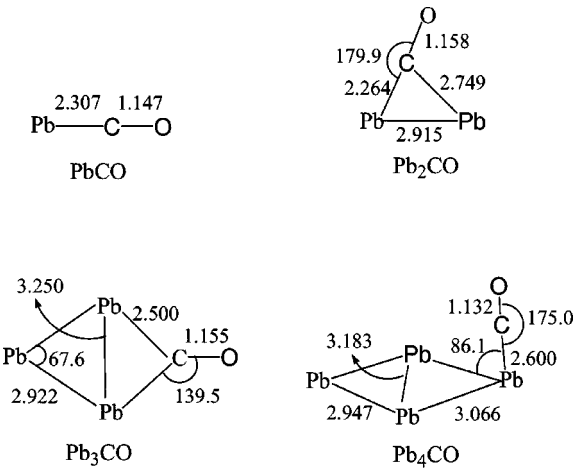

FIG. 4. Optimized structures (bond lengths in angstrom, bond angles in degree) of the reaction products.

B. Pb_nCO ($n=2-4$)

The present infrared spectra also provide evidence for the formation of small lead cluster carbonyls in the excess argon matrices. For instance, three new bands at 1915.5, 1923.8, and 2042.8 cm^{-1} are observed on sample annealing, which observably decrease upon broadband irradiation and almost recover on further annealing (Fig. 1). The IR spectra as a function of change of laser energies are of particular interest here (Fig. 2). When the laser power decreases from 5 to 4 mJ/pulse, the 2042.8 cm^{-1} band disappears. The yields of the 1915.5 and 1923.8 cm^{-1} bands decrease one by one with further decreasing the laser power.

Each band has some trapping site absorptions (Table I and Figs. 1–3) and we will focus on the main bands. These new bands shift to 1874.8, 1882.7, and 1998.8 cm^{-1} with $^{13}C\,^{16}O$, and to 1868.6, 1876.7, and 1993.2 cm^{-1} with

TABLE II. Ground electronic states, point groups, vibrational frequencies (cm^{-1}), and intensities (km/mol) of lead carbonyls calculated at the B3LYP/6-311+G(d)-LANL2DZ level.

Species	Ground electronic state	Point group	Frequency (intensity, mode)
PbCO	$^3\Sigma^-$	$C_{\infty v}$	1999.8 (1233, σ), 225.9 (2, σ), 221.9 (1×2, π)
Pb_2CO	$^1A'$	C_s	1921.7 (845,A'), 348.5 (18,A'), 289.8 (8,A''), 256.5 (3,A'), 122.4 (0.1,A'), 62.6 (1,A')
Pb_3CO	$^1A_1$	C_{2v}	1947.9 (1003,A_1), 326.7 (0,B_2), 307.0 (0,B_1), 199.9 (1,A_1), 131.3 (0,B_2), 125.4 (0.4,A_1), 98.0 (1,B_2), 92.2 (3,A_1), 47.2 (1,B_1)
Pb_4CO	$^1A'$	C_s	2133.0 (842,A'), 254.0 (6,A'), 193.5 (1,A''), 130.5 (4,A'), 113.6 (0.1,A'), 101.6 (0.3,A''), 87.9 (1,A'), 67.5 (1,A'), 52.9 (0.3,A''), 38.7 (2,A'), 29.3 (0,A'), 26.7 (0,A'')

$^{12}C\,^{18}O$, respectively. In the mixed $^{12}C\,^{16}O+{}^{13}C\,^{16}O$ and $^{12}C\,^{16}O+{}^{12}C\,^{18}O$, the 2042.8 cm^{-1} band is overlapped by the $^{13}C\,^{18}O$ absorption, and only pure isotopic counterparts are observed. The isotopic ratios ($^{12}C/^{13}C$: 1.0217, 1.0218, and 1.0220; $^{16}O/^{18}O$: 1.0251, 1.0251, and 1.0249, respectively) and mixed isotopic characteristic (Fig. 3) indicate that only one CO subunit is involved in these modes. Based on the laser power dependence of product yields, the absorptions at 1915.5, 1923.8, and 2042.8 cm^{-1} are assigned to the C–O stretching vibration of Pb_2CO, Pb_3CO, and Pb_4CO, respectively.

The assignments of the 1915.5, 1923.8, and 2042.8 cm^{-1} bands to $Pb_nCO\,(n=2-4)$ are strongly supported by the density functional calculations (Table II). The calculated frequencies are again in excellent agreement (only 0.3%, 1.3%, and 4.4% higher, respectively) with experimental values. As shown in Fig. 4, the optimized results predict that the most stable structures of Pb_2CO, Pb_3CO, and Pb_4CO include semibridge, bridge, and terminal-bonded carbonyls, respectively.

The optimized Pb–Pb distance in the naked Pb_2 cluster is 2.952 Å in accord with the previous relativistic calculations (2.94 Å) carried out by Balasubramanian and Pitzer.[17] The absorption for the Pb–Pb stretching of the Pb_2 cluster is IR inactive, whereas the vibrational frequency of Pb_2 was observed at 112 cm^{-1} in a study of emission and laser excitation spectra.[18] Bondybey and English reported the ground state of Pb_2 to be $X\,(O_g^+)$.[18] We find that Pb_2CO has an asymmetric structure with a $^1A'$ ground state (Table II and Fig. 4). There are two inequivalent Pb–C bond lengths in Pb_2CO (i.e., 2.264 and 2.749 Å). For Pb_2CO, the Pb–Pb bond length is 2.915 Å, which is 0.037 Å shorter than that of Pb_2.

The naked Pb_3 cluster has a $^3A_2'$ ground state with a triangle structure of D_{3h} symmetry, and the Pb–Pb bond length is 3.067 Å, which are in accordance with the previous studies.[39,40] The calculated results indicate that Pb_3CO has a $^1A_1$ ground state with two equivalent Pb–C bonds (2.500 Å). In Pb_3CO, the Pb–Pb bonds (2.922 and 3.250 Å) are 0.145 Å shorter and 0.183 Å longer than those of Pb_3 at the same DFT level.

For Pb_4, a planar rhombus arrangement with D_{2h} symmetry in the ^1A_g ground state is the most stable structure, in agreement with the previous studies.[21,39] The most stable structure of Pb_4CO is predicted to have a nonplanar geometry with C_s symmetry. The CO molecule is terminally bonded to one of the apex Pb atom of near rhombus Pb_4 and is nearly perpendicular to the Pb_4 plane. The C–O bond length in Pb_4CO (1.132 Å) is observably shorter than that in other lead carbonyls (1.147–1.158 Å), indicating that the interaction of CO with the Pb_4 cluster is the weakest among the lead carbonyls observed here.

To get insight into the CO dissociation energies for these lead carbonyls, we compute the binding energies between $Pb_n\,(n=2-4)$ and CO. Table IV lists the calculated results together with related properties. The CO binding energies for $Pb_n\,(n=2-4)$ are 22.60, 21.29, and 1.37 kcal/mol, respectively. In contrast to the aforementioned PbCO species, we note that the largest CO binding energy for lead carbonyl is Pb_2CO, closely followed by Pb_3CO, and then by PbCO, and

TABLE III. Comparison of the observed and calculated isotopic frequency ratios of the reaction products.

		$^{12}C/^{13}C$		$^{16}O/^{18}O$	
Molecule	Mode	Obs	Calc	Obs	Calc
PbCO	C–O stretching	1.0221	1.0224	1.0250	1.0252
Pb_2CO	C–O stretching	1.0217	1.0225	1.0251	1.0252
Pb_3CO	C–O stretching	1.0218	1.0222	1.0251	1.0254
Pb_4CO	C–O stretching	1.0220	1.0226	1.0249	1.0251

TABLE IV. Net charges of CO (q_{CO}), selected bond lengths of $M-C$ and C–O, vibrational frequencies of C–O stretching mode, and CO binding energies (E_b) calculated at the B3LYP/6-311+G(d)-LANL2DZ level.

Species	Spin	q_{CO}	R_{M-C} (Å)	R_{C-O} (Å)	ν_{C-O} (cm^{-1})	E_b (kcal/mol)
CO	0	0.000		1.128	2211.4	
PbCO	1	−0.190	2.307	1.147	1999.8	16.12
Pb_2CO	0	−0.290	2.264	1.158	1921.7	22.60
Pb_3CO	0	−0.231	2.500	1.155	1947.9	21.29
Pb_4CO	0	−0.027	2.600	1.132	2133.0	1.37

the smallest one is Pb_4CO, suggesting that the activation of CO by Pb_n ($n=1-4$) is in the order $Pb_2CO > Pb_3CO > PbCO > Pb_4CO$. Also, the strength of CO binding with Pb_n ($n=1-4$) is well exhibited by the observed and calculated vibrational frequencies of C–O stretching mode and C–O bond lengths in Pb_nCO carbonyls. In addition, the net charges of CO presented in Table IV show that the partial electron is transferred from Pb_n ($n=1-4$) to CO, where Pb_n behaves as a donor while CO behaves as an acceptor in bonding between Pb_n and CO.

C. Reaction mechanisms

At the present experimental conditions, lead atoms seem to be the predominant species produced from the laser ablation of the lead target. No primary lead carbonyl species are formed on sample deposition. The laser-ablated lead atoms react with CO molecules upon annealing in the excess argon matrices to produce PbCO as well as small lead cluster carbonyls Pb_nCO ($n=2-4$).

Table V presents the energetics for possible reactions of lead atoms with CO molecules calculated at the B3LYP/6-311+G(d)-LANL2DZ level. The reaction 1 is exothermic (−38.30 kcal/mol), indicating that the formation of Pb_2 cluster from two $Pb(^3P_0)$ atoms is very favorable, which is consistent with the previous observations.[17,18,41] Successive formation of Pb_3 and Pb_4 clusters is more exothermic than that of Pb_2. The present DFT calculations strongly imply that the formation of these small lead clusters from Pb atoms is attainable, for which some weak absorptions are expected to appear in far-infrared spectra.

The PbCO carbonyl appears on sample annealing, disappears on broadband irradiation, and recovers on further annealing, suggesting that the generation of PbCO is exothermic with some activation energy, in agreement with the calculated reaction energy (reaction 5, −16.12 kcal/mol). It can be found from Table V that the two pathways (reactions 7 and 8) for the formation of Pb_2CO carbonyl (reaction energy: −22.60 and −39.82 kcal/mol) are both more exothermic than that for $Pb(CO)_2$ (−2.44 kcal/mol). The CO addition to PbCO to produce $Pb(CO)_2$ seems to be less favorable even at high CO concentrations, which is consistent with the absence of the $Pb(CO)_2$ absorption.

We also note that the absorption of Pb_3CO carbonyl appears after Pb_2CO. It can be inferred that the contributions to the formation of Pb_3CO are mainly from the reactions of PbCO with Pb_2 (reaction 10, −60.08 kcal/mol) and Pb_2CO with Pb atom (reaction 11, −58.56 kcal/mol), while the contribution from the reaction 9 cannot be excluded. The latest observation of the Pb_4CO absorption indicates that the generation of Pb_4CO carbonyl may be mainly from reactions 13, 14, and 15, whereas the contribution from reaction 12 seems to be of minor importance.

IV. CONCLUSIONS

Laser-ablated Pb atoms react with CO molecules on annealing in excess argon to produce the lead carbonyls,

TABLE V. Energetics for possible reactions of lead atoms with CO calculated at the B3LYP/6-311+G(d)-LANL2DZ level.

Reaction		Reaction energy[a] (kcal/mol)
1	$Pb(^3P_0)+Pb(^3P_0) \rightarrow Pb_2[X(O_g^+)]$	−38.30
2	$Pb_2[X(O_g^+)]+Pb(^3P_0) \rightarrow Pb_3(^3A_2')$	−56.52
3	$Pb_2[X(O_g^+)]+Pb_2[X(O_g^+)] \rightarrow Pb_4(^1A_g)$	−83.62
4	$Pb_3(^3A_2')+Pb(^3P_0) \rightarrow Pb_4(^1A_g)$	−65.40
5	$Pb(^3P_0)+CO \rightarrow PbCO(^3\Sigma^-)$	−16.12
6	$PbCO(^3\Sigma^-)+CO \rightarrow Pb(CO)_2(^1A_1)$	−2.44
7	$Pb_2[X(O_g^+)]+CO \rightarrow Pb_2CO(^1A')$	−22.60
8	$PbCO(^3\Sigma^-)+Pb(^3P_0) \rightarrow Pb_2CO(^1A')$	−39.82
9	$Pb_3(^3A_2')+CO \rightarrow Pb_3CO(^1A_1)$	−21.29
10	$PbCO(^3\Sigma^-)+Pb_2[X(O_g^+)] \rightarrow Pb_3CO(^1A_1)$	−60.08
11	$Pb_2CO(^1A')+Pb(^3P_0) \rightarrow Pb_3CO(^1A_1)$	−58.56
12	$Pb_4(^1A_g)+CO \rightarrow Pb_4CO(^1A')$	−1.37
13	$PbCO(^3\Sigma^-)+Pb_3(^3A_2') \rightarrow Pb_4CO(^1A')$	−50.65
14	$Pb_2CO(^1A')+Pb_2[X(O_g^+)] \rightarrow Pb_4CO(^1A')$	−67.35
15	$Pb_3CO(^1A_1)+Pb(^3P_0) \rightarrow Pb_4CO(^1A')$	−47.09

[a]A negative value of energy denotes that the reaction is exothermic.

$Pb_nCO\,(n=1-4)$. The absorptions at 2027.7 and 1915.5 cm^{-1} are assigned to C–O stretching modes of PbCO and Pb_2CO, respectively. Further reactions lead to the formation of Pb_3CO (1923.8 cm^{-1}) and Pb_4CO (2042.8 cm^{-1}). Pb_2CO and Pb_3CO are bridge-bonded carbonyl compounds, whereas Pb_4CO is a terminal-bonded carbonyl molecule. The observation of $Pb_nCO\,(n=1-4)$ is in good agreement with the prediction of density functional theory calculations. The calculated CO binding energies for $Pb_nCO\,(n=1-4)$ follow the order $Pb_2CO > Pb_3CO > PbCO > Pb_4CO$, in accord with the observed infrared frequencies of C–O stretching.

ACKNOWLEDGMENTS

The authors gratefully acknowledge financial support for this research from AIST and Kobe University. They wish to thank Professor M. F. Zhou for valuable discussions. L.J. acknowledges JASSO and Kobe University for Honors Scholarship.

[1] M. F. Zhou, L. Andrews, and C. W. Bauschlicher, Jr., Chem. Rev. (Washington, D.C.) **101**, 1931 (2001).
[2] H. J. Himmel, A. J. Downs, and T. M. Greene, Chem. Rev. (Washington, D.C.) **102**, 4191 (2002).
[3] L. N. Zhang, J. Dong, M. F. Zhou, and Q. Z. Qin, J. Chem. Phys. **113**, 10169 (2000); Q. Y. Kong, M. H. Chen, J. Dong, Z. H. Li, K. N. Fan, and M. F. Zhou, J. Phys. Chem. A **106**, 11709 (2002); L. Miao, L. M. Shao, W. N. Wang, K. N. Fan, and M. F. Zhou, J. Chem. Phys. **116**, 5643 (2002); L. N. Zhang, J. Dong, and M. F. Zhou, Chem. Phys. Lett. **334**, 335 (2001).
[4] M. E. Jacox, D. E. Milligan, N. G. Moll, and W. E. Thompson, J. Chem. Phys. **43**, 3734 (1965).
[5] L. N. Zhang, J. Dong, and M. F. Zhou, J. Chem. Phys. **113**, 8700 (2000).
[6] C. Devillers and D. A. Ramsay, Can. J. Phys. **49**, 2839 (1971).
[7] S. P. Walch, J. Chem. Phys. **72**, 5679 (1980).
[8] W. M. Pitts, V. M. Donnelley, A. P. Baronavski, and J. R. McDonald, Chem. Phys. **61**, 451 (1981).
[9] R. J. Van Zee, R. F. Ferrante, and W. Weltner, Jr., Chem. Phys. Lett. **139**, 426 (1987).
[10] S. P. Walch, J. Chem. Phys. **72**, 5679 (1980).
[11] Y. Ohshima and Y. Endo, J. Chem. Phys. **102**, 1493 (1994).
[12] R. L. DeKock, R. S. Grev, and H. F. Schaefer, J. Chem. Phys. **89**, 3016 (1988).
[13] Z. L. Cai, Y. F. Wang, and H. W. Xiao, Chem. Phys. Lett. **191**, 533 (1992).
[14] H. U. Suter, M. B. Huang, and B. Engels, J. Chem. Phys. **101**, 7686 (1994).
[15] A. Feltrin, S. N. Cesaro, and F. Ramondo, Vib. Spectrosc. **10**, 139 (1996).
[16] R. R. Lembke, R. F. Ferrante, and W. Weltner, Jr., J. Am. Chem. Soc. **99**, 416 (1977); A. D. Walters, W. Winnewisser, K. Lattner, and B. P. Winnewisser, J. Mol. Spectrosc. **149**, 542 (1991).
[17] K. Balasubramanian and K. S. Pitzer, J. Chem. Phys. **78**, 321 (1983).
[18] V. E. Bondybey and J. H. English, J. Chem. Phys. **67**, 3405 (1977).
[19] A. Hoareau, P. Melinon, B. Cabaud, D. Rayne, B. Tribollet, and M. Broyer, Chem. Phys. Lett. **143**, 602 (1988).
[20] J. Ho, M. Polak, and W. C. Lineberger, J. Chem. Phys. **96**, 144 (1992).
[21] D. G. Dai and K. Balasubramanian, J. Chem. Phys. **96**, 8345 (1992).
[22] B. Tremblay, G. Gutsev, L. Manceron, and L. Andrews, J. Phys. Chem. A **106**, 10525 (2002).
[23] M. F. Zhou, G. V. Chertihin, and L. Andrews, J. Chem. Phys. **109**, 10893 (1998).
[24] M. F. Zhou and L. Andrews, J. Chem. Phys. **110**, 10370 (1999).
[25] B. Tremblay, L. Manceron, G. Gutsev, L. Andrews, and H. Partridge III, J. Chem. Phys. **117**, 8479 (2002).
[26] M. F. Zhou, Z. X. Wang, P. von Ragué Schleyer, and Q. Xu, ChemPhysChem **4**, 763 (2003).
[27] M. F. Zhou, L. Jiang, and Q. Xu, J. Chem. Phys. **121** (2004).
[28] G. L. Gutsev, C. W. Bauschlicher, Jr., and L. Andrews, J. Chem. Phys. **119**, 3681 (2003).
[29] Z. X. Cao, Y. J. Wang, J. Zhu, W. Wu, and Q. E. Zhang, J. Phys. Chem. B **106**, 9649 (2002).
[30] I. S. Ignatyev, H. F. Schaefer III, R. B. King, and S. T. Brown, J. Am. Chem. Soc. **122**, 1989 (2000).
[31] T. R. Burkholder and L. Andrews, J. Chem. Phys. **95**, 8697 (1991); M. H. Chen, X. F. Wang, L. N. Zhang, M. Yu, and Q. Z. Qin, Chem. Phys. **242**, 81 (1999); M. F. Zhou, N. Tsumori, L. Andrews, and Q. Xu, J. Phys. Chem. A **107**, 2458 (2003).
[32] M. J. Frisch, G. W. Trucks, H. B. Schlegel *et al.*, GAUSSIAN03, Revision B.04, Gaussian, Inc., Pittsburgh, PA, 2003.
[33] A. D. Becke, J. Chem. Phys. **98**, 5648 (1993).
[34] C. Lee, E. Yang, and R. G. Parr, Phys. Rev. B **37**, 785 (1988).
[35] A. D. McLean and G. S. Chandler, J. Chem. Phys. **72**, 5639 (1980); R. Krishnan, J. S. Binkley, R. Seeger, and J. A. Pople, *ibid.* **72**, 650 (1980).
[36] J. H. Wachter, J. Chem. Phys. **52**, 1033 (1970); P. J. Hay, *ibid.* **66**, 4377 (1977).
[37] P. J. Hay and W. R. Wadt, J. Chem. Phys. **82**, 299 (1985).
[38] We have performed the DFT calculations at the B3LYP/6-311+G(d)-LANL2DZ level for all the possible isomers of $Pb_nCO\,(n=1-4)$. The calculated results show that the linear Pb–Pb–CO ($^1\Sigma^-$, $C_{\infty v}$, $R_{C-O}=1.145$ Å, $\nu_{C-O}=2021.3\ cm^{-1}$) with two imaginary frequencies (-61.7 and $-61.7\ cm^{-1}$) lies 25.98 kcal/mol above the most stable, semibridged Pb_2CO ($^1A'$, C_s, 1.158 Å, 1921.7 cm^{-1}). The terminally bonded structure of Pb_3CO ($^1A_1$, C_{2v}, 1.128 Å, 2212.1 cm^{-1}) with four imaginary frequencies (-13.5, -13.2, -1.0, and $-0.9\ cm^{-1}$) lies 21.30 kcal/mol above the most stable, bridge-boned one ($^1A_1$, C_{2v}, 1.155 Å, 1947.9 cm^{-1}). Furthermore, the planar Pb_4CO structure ($^1A_1$, C_{2v}, 1.155 Å, 1958.7 cm^{-1}) with one imaginary frequency ($-542.8\ cm^{-1}$) lies 48.07 kcal/mol above the most stable one ($^1A'$, C_s, 1.132 Å, 2133.0 cm^{-1}). Mainly the results of the most stable structures are presented for discussions.
[39] D. D. Stranz and R. K. Khanna, J. Chem. Phys. **74**, 2116 (1981).
[40] K. Balasubramanian and D. Majumdar, J. Chem. Phys. **115**, 8795 (2001).
[41] V. E. Bondybey and J. H. English, J. Chem. Phys. **76**, 2165 (1982).